Chapter 4

Biosorption of dyes

Jindrayani Nyoo Putro[a], Yi-Hsu Ju[b,c], Felycia Edi Soetaredjo[d], Shella Permatasari Santoso[d], Suryadi Ismadji[d]

[a]*Department of Chemical Engineering, National Taiwan University of Science and Technology, Taipei City, Taiwan;* [b]*Graduate Institute of Applied Science and Technology, National Taiwan University of Science and Technology, Taipei City, Taiwan;* [c]*Taiwan Building Technology Center, National Taiwan University of Science and Technology, Taipei City, Taiwan;* [d]*Department of Chemical Engineering, Widya Mandala Surabaya Catholic University, Surabaya, East Java, Indonesia*

1. Introduction

Contamination of the aquatic environment by dyestuffs causes severe problems for humans and aquatic biota. Environmental problems caused by the pollution of dyestuffs become more complicated because most of the dyes discharged into the environment are synthetic dyes. Mostly, these synthetic dyes are designed to be resistant to degradation by microorganisms. Once the synthetic dyes release into the environment, it will resist biological degradation for a long time. Therefore, a treatment process should be conducted before the wastewater containing dyes releases to the water environment. Currently, several processes for the treatment of the wastewater containing dyes are available. In terms of effectiveness, the adsorption process is the most suitable method for treating wastewater containing dyes, especially at low concentrations. The success of treating wastewater containing dyes using the adsorption process is highly dependent on the adsorption capacity of the adsorbent used.

The use of a variety of environmentally friendly and inexpensive adsorbents to remove dyes from water or wastewater has been studied by thousands of researchers in the last few decades. Several current review articles discussed the removal of dyes from water or wastewater and are also available in the scientific journal publications (Shamsollahi and Partovinia, 2019; Zhou et al., 2019; Afroze and Sen, 2018; Anastopoulos et al., 2017; Bhatnagar et al., 2010, 2015; Anastopoulos; Kyzas, 2014). These environmentally friendly and inexpensive adsorbents include agricultural wastes and its modified forms, seeds and leaves of various plants, industrial by-products, different kinds of microorganisms (living or dry ones), and natural polymer composites.

The studies of dyes removal using biosorbents have been conducted for more than three decades; however, the biosorption study still very attractive for the scientists indicated by a large number of publications in this area in recent years. Newly modified biosorbents including multifunctional and composite biosorbents have been prepared and used for the color removal from aqueous solutions. Therefore, reviews about the current progress of dyes biosorption are still required. This chapter summarizes and discusses the up-to-date progress of biosorption of dyes using newly modified biosorbents. Various aspects of dyes biosorption are given and comprehensively explained.

2. Classification of synthetic dyes

Synthetic dyes are developed to fulfill the human needs of modern and biologically and physically resistant coloring agents. Usually, synthetic dyes are classified according to their application, chemical structure, ionic forms in the solution, as well as its color (Zhou et al., 2019). Classification of dyes based on their chemical structure possibly is the most appropriate way since it offers many advantages (Gregory, 1990). Based on this method of classification, dyes can be categorized as follow:

- Azo dyes: CI disperse yellow 16, CI solvent yellow 14, disperse blue, reactive brown, CI acid black 1, CI direct green 26, etc.
- Anthraquinone dyes: quanizarin, CI disperse red 15, CI disperse violet 1, disperse torquise, etc.
- Benzodifurano dyes: disperse red.
- Polycyclic aromatic carbonyl dyes (anthraquinonoid vat dyes): the blue, indanthrone, CI vat black, the green, the brown, etc.
- Indigoid dyes: tyrian purple.
- Polymethine and related dyes: cyanine, carbocyanine, azacarbocyanines, etc.
- Styryl dyes: malononitrile, CI disperse yellow 31, dicyanovinyl dyes, tetracyanoethylene, etc.
- Di and tri-aryl carbonium and related dyes: diarylcarbonium dyes, malachite green, CI basic blue 9, etc.
- Phthalocyanines dyes: CI direct blue 86, hemin, etc.
- Quinophthalone dyes: CI solvent yellow 33, CI disperse yellow 54, etc.
- Sulfur dyes: CI sulfur black 1.
- Nitro and nitroso dyes: CI acid yellow 1, CI 10,305, CI disperse yellow 14, CI acid green 1, etc.
- Miscellaneous dyes: stilbene dyes, formazan dyes.

Details about properties, synthesis, and structures of synthetic dyes can be seen elsewhere (Gregory, 1990).

3. Agricultural and plant wastes as biosorbents

A variety of agricultural and plant wastes have been employed as cheap adsorbents for the removal of various dyes from aqueous solutions as listed in Table 4.1. Some of the biomass has potential application for the industrial-scale wastewater treatment process, while others possibly will end up only in the laboratory-scale application. The low adsorption capacity of agricultural and plant wastes materials is the main obstacle of using these alternative adsorbents for the industrial-scale treatment of wastewater containing dyes.

TABLE 4.1 Adsorption of various dyes using agricultural and plant wastes.

Agricultural waste	Dyes	Adsorption capacity, mg/g	Reference
Azolla filiculoides	Basic orange	833 at pH 7 and T = 30 °C	Tan et al. (2010)
Brazil nutshells	Methylene blue (MB) and indigo carmine (IC)	7.81 (MB), and 1.09 (IC)	Brito et al. (2010)
Chia seeds (*Salvia hispanica*)	Reactive yellow B2R	70.95 at pH 2 and T = 30°	Da Silva and Pietrobelli (2019)
Corn silk	Reactive blue 19 (RB19) and reactive red 218 (RR218)	71.6 (RB19) and 63.3 (RR218) at pH 2.0 and T = 25 °C	Degermenci et al. (2019)
Elaeagnus angustifolia L. fruits	Methylene blue (MB), and Indigo Carmine (IC)	344.8 (MB) and 9.7 (IC) at room temperature	Oymak and Eruygur (2019)
Glossogyne tenuifolia leaves	Congo red (CR) and malachite green (MG)	13.4 (CR), and 210.9 (MG) at T = 40 °C	Yang and Hong (2018)
Mentha pulegium	Direct Red 80 (DR80) and Acid Black 26 (AB26)	52.3 (DR80) and 46.3 (AB26) at pH 2.5 and T = 25 °C	Mahmoodi et al. (2011)
Moringa oleifera seed	Reactive red 120	413.32 at T = 50 °C and pH 1.0	Celekli et al. (2019)
Musa acuminate peel	Emerald green	10.75 at T = 25 °C	Rehman et al. (2019)
Olive stone	Alizarin Red S (ARS), and methylene blue (MB)	16.10 (ARS), and 13.2 (MB)	Albadarin and Mangwandy (2015)

TABLE 4.1 Adsorption of various dyes using agricultural and plant wastes.—cont'd

Agricultural waste	Dyes	Adsorption capacity, mg/g	Reference
Orange bagasse	Reactive blue 5G	28.9 at T = 40 °C	Fiorentin et al. (2010)
Palm date stones	Basic violet 3 (BV3), and Basic red 2 (BR2)	97.8 (BR2) and 117.3 (BV3) at pH 7.7 and T = 35 °C	Wakkel et al. (2019)
Palm kernel fiber	Methyl violet	114.2 at T = 66 °C	Ofomaja et al. (2011)
Parthenium hysterophorus L	Safranine	89.3 at pH 6	Shrivastava (2010)
Paulownia tomentosa stud leaf powder	Acid Orange 52	10.5 at T = 25 °C	Deniz and Saygideger (2010)
Pinus sylvestris L	Reactive red 195	6.69 at 20 °C, and 7.38 at 50 °C	Aksakal and Ucun (2010)
Pine tree leaves	Basic red 46	71.94 at T = 45 °C	Deniz and Karaman (2011)
Princess tree leaves	Basic red 46	43.10 at T = 45 °C	Deniz and Saygideger (2011)
Rice husk	Direct red 31 (DR31) and Direct orange 26 (DO26)	57.88 (DR31) at pH 2, and 36.14 (DO26) at pH 3, adsorption temperature was 30 °C	Safa and Bhatti (2011)
Sapindus mukorossi dead leaves	CI Reactive red 241	8.18 at T = 30 °C	Javed et al. (2019)
Sesame hull	Methylene blue	359 at T = 30 °C	Feng et al. (2011)
Solanum tuberosum peel	Emerald green	2.61 at T = 25 °C	Rehman et al. (2019)
Soybean hulls	BF−4B reactive red	19 at pH 1 and T = 45 °C	Módenes et al. (2019)
Walnut shell	Methylene blue	80.4 at T = 45 °C	Liu et al. (2019)
Water hyacinth leaves	Amaranth dye	70 at pH = 1.5 and T = 50 °C	Guerrero-Coronilla et al. (2015)

Agricultural and plant wastes biomass are categorized as lignocellulosic materials which are mainly composed of lignins, hemicellulose, and cellulose. Lignins are composed of benzene derivatives such as coumaryl, sinapyl, and coniferyl alcohols, and it has very complex and variable structures. Hemicelluloses are sugar polymers that consist of C_5 and C_6 sugar monomers. The polymerization degree in hemicelluloses is lower than celluloses. While celluloses are polysaccharides which consist of a linear chain of β-1,4-linked D-glucose monomers. The composition of lignins, hemicellulose, and celluloses in the lignocellulosic materials strongly depends on the type of biomass, geographic condition, and also season. The chemical composition variation of agricultural and plant wastes is another big challenge of using these lignocellulosic materials as the industrial biosorbents.

Low Brunauere-Emmere-Teller (BET) surface area as well as small pore volume are the characteristics of lignocellulosic materials. With this poor pore structure, natural lignocellulosic materials usually possess small adsorption capacity toward a particular type of dyes (Aksakal and Ucun, 2010; Brito et al., 2010; Deniz and Saygideger, 2010, 2011; Fiorentin et al., 2010; Albadarin and Mangwandy, 2015; Yang and Hong, 2018; Javed et al., 2019; Módenes et al., 2019; Rehman et al., 2019). Typical nitrogen sorption isotherm of agricultural waste material (cassava peel) is given in Fig. 4.1. However, in some cases, the excellent adsorption capacity was observed for some natural lignocellulosic materials (Tan et al., 2010; Celekli et al., 2019;
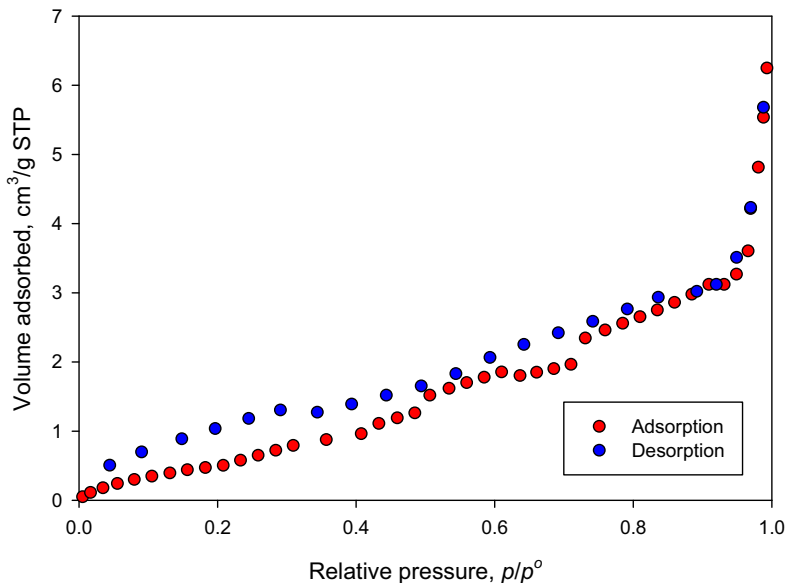

FIG. 4.1 Sorption isotherms of nitrogen onto cassava peel waste.

Oymak and Eruygur, 2019). The natural lignocellulosic materials have high adsorption capacity possible due to the excess presence of polar functional group-containing compounds (Lesmana et al., 2009). In the adsorption of dyes using lignocellulosic materials, particular surface functional groups of adsorbent play an essential role. These functional groups are likely responsible for binding with dyes molecules during the adsorption process.

Several polar and nonpolar functional groups which usually exist in the agricultural waste materials are as follow: $O - H$ stretch (alcohols or phenols), $N - H$ stretch ($1°$ and $2°$ amines), $C - H$ stretch (methylenes), $C = O$ stretch (carboxylic acids, saturated aliphatic esters, carboxyls), $C = C$ stretch (alkynes), and $C - H$ bend (aromatic compounds). The existence of surface functional groups on the agricultural waste usually is obtained using a Fourier Transform Infra-Red (FTIR) method. In the case of the adsorption of reactive red 120 on *Moringa oleifera* seed, the carbonyl, amines, and amide groups play essential roles in the binding of the dye (Çelekli et al., 2019).

4. Thermal modification of agricultural wastes

To increase the adsorption capacity of some agricultural waste toward dyes molecules, the modification at high temperatures is one of the best options. During the thermal treatment, the lignocellulosic materials will be decomposed into some low molecular weight compounds (gases and tar) and leaving solid carbonaceous material known as biochar or the black product. The resulting biochar possesses a porous structure; however, in many cases, the direct use of this solid material as the adsorbent often gives unsatisfactory results. Activation using some chemicals (known as chemical activation) or oxidizing gases (physical activation) usually is conducted to increase the adsorption capacity of the biochar/activated carbon (Table 4.2).

Thermal modification of lignocellulosic materials (physical or chemical) produces porous materials known as activated carbons or activated biochars. Thermal modification using chemicals as the activating agent offers several advantages than the physical one (Sudaryanto et al., 2006), such as

- Lower temperature, usually between 400 and 600 °C.
- The single-step process, the activation, and the carbonization process take place in one process.
- The chemical activation process produces a higher yield of solid than physical activation.

The main drawback of the modification of lignocellulosic materials using chemical agents is often, it produces hazardous wastewater (depends on the chemical agents used), which creates another environmental problem. The physical activation is known as an environmentally friendly process since it only utilizes steam or carbon dioxide as the activating agent.

TABLE 4.2 Thermal process of some agricultural and plant wastes.

Agricultural waste	Thermal process	Application	Reference
Almond shell	Microwave-assisted process	Methylene blue adsorption	Du et al. (2016)
Coconut shell	Thermochemical activation process using $ZnCl_2$ at 700 °C	Adsorption of methylene blue, malachite green, and methyl orange	Gupta and Khatri (2019)
Corncob	Steam activation at 892 °C for 40 min	Methylene blue adsorption	Yu et al. (2019)
Corn stigmata	Hydrothermal carbonization at 180 °C followed by CO_2 activation at 900 °C	Methylene blue adsorption	Mbarki et al. (2019)
Foxtail palm	Vacuum pyrolysis at 400 −700 °C and activated using H_2SO_4, H_3PO_4, and KOH	Methylene blue adsorption	Dos Santos et al. (2019)
Mangosteen peel	$ZnCl_2$ activation at 600 °C	Methylene blue adsorption	Nasrullah et al. (2019)
Olive tree pruning and coffee husk	Chemical activation at 500 °C (K_2CO_3 and KOH), and physical activation at 910 °C (steam)	Methylene blue adsorption	Mamani et al. (2019)
Peanut shell	Carbonized at 800 °C in the presence of $FeCl_3$ in CO_2 environment	Malachite green adsorption	Guo et al. (2018)
Pineapple crown leaf	Carbonization at 500 °C followed by chemical activation (KOH) using microwave irradiation	Methyl violet adsorption	Astuti et al. (2019)
Pinecone	Pyrolized at 500 °C and activated using $ZnCl_2$	Alizarin red S adsorption	Bhomic et al. (2018)
Pinecone	Microwave-induced $ZnCl_2$ activation	Methylene blue adsorption	Ozhan et al. (2014)
Prickly pear seeds and cactus	Activated using H_3PO_4 at the temperature of 450 °C	Methylene blue adsorption	Ouhammou et al. (2019)
Shiitake mushroom	Activated using K_2CO_3 and carbonized at 800 °C	Methylene blue adsorption	Sun et al. (2019)

TABLE 4.2 Thermal process of some agricultural and plant wastes.—cont'd

Agricultural waste	Thermal process	Application	Reference
sunflower seed husk	ZnCl$_2$ was used as a chemical activating agent, and the carbonization was conducted at 500 °C using microwave irradiation as the heat source	Methylene blue adsorption	Baytar et al. (2018)
Walnut shell	Activated with phosphoric acid and carbonized at 450 °C	Malachite green adsorption	Hajialigol and Masoum (2019)
Water fern	Carbonized at 300 °C, and activated using NaOH and KOH and followed by activation at 600 °C under argon atmosphere for 3 h	Acid orange II adsorption	Emrooz et al. (2019)

In the thermal activation process, several steps of processes occurred during the heating process that leads to the pore creation. The first step of the methods is the release of free moisture content and bound water from the structure of lignocellulosic material. The evaporation of both free and bound water occurs at a temperature of around 50−200 °C. In the subsequent step of the processes, which occur at a temperature range of 200−300 °C, the hemicellulose will disappear due to the decomposition. At higher temperatures (300−360 °C), the cellulose decomposes into the smaller molecular weight of organic compounds, and the last part of organic substance in the lignocellulosic material, lignin, will decompose at a temperature of 360−500 °C. The degradation or decomposition of high molecular weight compounds into the smaller ones of the structure of lignocellulosic material will create space within the internal structure of the material. The creation of space in the internal structure of materials will increase the active surface area of the materials and later will enhance its adsorption performance.

Chemical and physical activation processes were employed by Mamani et al. (2019) to prepare the activated carbons from the coffee husk and olive tree pruning. The impregnation of the biomasses was conducted at 130 °C using potassium hydroxide (KOH) and potassium carbonate (K$_2$CO$_3$) as chemical activating agents, and the activation was performed at 800 °C. For physical activation, the carbonization was conducted at 500 °C and the gasification at 910 °C using superheated steam as the activating agent.

The chemical activation produced the carbon with a surface area over 2500 m^2/g, while for the physical process created carbon with BET surface area around 1500 m^2/g. The resulting carbons could remove more than 99% of methylene blue from aqueous solution.

5. Combination of agricultural wastes and other lignocellulosic materials with other materials to form composites

To enhance the adsorption capacity of the activated carbon derived from the agricultural waste, the combination with other materials was usually performed to produce new composite materials which have high adsorption performance or capacity. Naushad et al. (2019) developed arginine-modified−activated carbon (AGDPA@AC) for removal of methylene blue from aqueous solution. The maximum uptake of methylene blue by the AGDPA@AC was achieved at pH 8 and temperature of 25 °C (219.9 mg/g). The time required to reach the equilibrium condition was 120 min.

The combination of macroalgae *Saccharina japonica* (which is also known as kelp) with montmorillonite to form the composite of biochar−bentonite was studied by Sewu et al. (2019). The composite was utilized as the adsorbent for the removal of an anionic dye (Congo Red) and cationic dye (crystal violet). The incorporation of bentonite into biochar increased its mesopores structure, and it enhanced the adsorption performance of the composite material toward the Congo Red and crystal violet (at 30 °C).

6. Algae as biosorbents

Many research groups around the world have conducted studies on the removal of dyes from water or wastewater using microalgae as well as macroalgae for many years. Their adsorption capability and its abundant availability as diverse groups of plant-like organisms which can be found easily as either in multicellular or unicellular forms make these organisms very attractive as the alternative low-cost biosorbents (Table 4.3).

Sargassum dentifolium and Ulva fasciata (macroalgae species) have been tested for their adsorption performance to remove methylene blue from aqueous solution by Moghazy et al. (2019). There is high removal efficiency for both macroalgae due to the presence of various surface functional groups that possess high adsorption affinity toward methylene blue molecule. Different adsorption mechanisms between the surface functional groups of macroalgae with methylene blue cation occurred during the adsorption process, such as ionic interaction, coordination, ion-dipole bond, and van der Waals interaction (Moghazy et al., 2019).

Brown macroalgae *Stoechospermum marginatum* was utilized to recover Acid Blue 25, Acid Orange 7, and Acid Black 1 (acid dyes) from the aqueous

TABLE 4.3 Adsorption of dyes using algae as biosorbents.

Algae	Dye	Parameters	Adsorption capacity, mg/g	Reference
Chlorella pyrenoidosa	Direct Red-31	pH: 3–14; contact time: 0–180 min; initial dye concentration: 10–50 mg/L	30.53	Sinha et al. (2016)
	Methylene blue	pH: 6; temperature: 28 °C; time: 24 h; initial concentration of dye: 100 mg/L	101.75	Lebron et al. (2018)
	Rhodamine B	pH: 2–10; temperatures: 25, 35, 45 °C; contact time: 5–240 min; initial dye concentration: 100 mg/L	63.14	Da Rosa et al. (2018)
	Methylene blue	Modified with H_3PO_4 and $ZnCl_2$; pH: 6; temperature: 28 °C; adsorbent dose: 2 g/L	212	Lebron et al. (2019)
Chlorella vulgaris	Supranol Red 3BW, Lanaset Red 2 GA, and Levafix Navy Blue EBNA	pH: 3.85–11.40; temperature: 35–58 °C	256.4 (Supranol Red 3BW), 345 (Lanaset Red 2 GA), and 188.7 (Levafix Navy Blue EBNA)	Lim et al. (2010)
Enteromorpha prolifera	Direct Fast Scarlet 4BS	pH: 0.5–10; temperature: 30–50 °C; time: 5–540 min	318.87	Sun et al. (2019)
Fucus vesiculosus	Methylene blue	Modified with H_3PO_4 and $ZnCl_2$; pH: 6; temperature: 28 °C; adsorbent dose: 2 g/L	1162.9	Lebron et al. (2019)
Laminaria japonica	Methylene blue	pH: 2–10; temperature: 25 °C; time: 0–60 min; adsorbent dose: 0.2–2.0 g/L	549.45	Shao et al. (2017)

Sargassum dentifolium	Methylene blue	pH: 3–9; temperature: 20–50 °C; biosorbent dose: 0.25–3 g/L; contact time: 0–90 min; initial concentration of dye: 20–80 mg/L	66.6	Moghazy et al. (2019)
Spirulina maxima	Methylene blue	pH: 6; temperature: 28 °C; time: 24 h; initial concentration of dye: 100 mg/L	145.34	Lebron et al. (2018)
	Methylene blue	Modified with H_3PO_4 and $ZnCl_2$; pH: 6; temperature: 28 °C; adsorbent dose: 2 g/L	343.66	Lebron et al. (2019)
Stoechospermum marginatum	Acid Blue 25, Acid Orange 7, and Acid Black 1	pH: 2–10; temperature 27 °C; initial dye concentration: 10–50 mg/L	22.2 (Acid Blue 25); 6.73 (Acid Orange 7), and 6.57 (Acid Black 1)	Daneshvar et al. (2012)
Ulothrix sp.	Methylene blue	pH: 1.3–10.4; temperature: 20–60 °C; biosorbent dose: 0.5–5 g/L; contact time: 0.5–12 h.	86.1	Dogar et al. (2010)
Ulva fasciata	Methylene blue	pH: 3–9; temperature: 20–50 °C; biosorbent dose: 0.25–3 g/L; contact time: 0–90 min; initial concentration of dye: 20–450 mg/L	244	Moghazy et al. (2019)

solution by Daneshvar et al. (2012). Various operation parameters (pH, temperature, initial concentration of acid dyes, the particle size of biosorbent, and contact time) influence the uptake of acid dyes by *Stoechospermum marginatum*. The maximum adsorption capacities of the brown macroalgae were 6.57.6.73, and 22.2 mg/g for Acid Black 1, Acid Orange 7, and Acid Blue 25. The low adsorption capacity of brown macroalgae *Stoechospermum marginatum* toward acid dyes is due to the lack of internal micropore and mesopore structures in brown macroalgae. The adsorption of acid dyes solely occurred in the macropore structure and several surface functional groups available on the surface of the macroalgae. The FTIR analysis reveals that the amine and hydroxyl groups are mainly responsible for the uptake of the acid dyes.

Ulothrix species is a filamentous green alga which is widely found in both marine and freshwater. This species of algae had been studied for its possibility as an alternative adsorbent for methylene blue removal from aqueous solution (Dogar et al., 2010). The adsorption capability of the Ulothrix species toward methylene blue was strongly influenced by the pH of the solution and temperature of the system. The adsorption capacity of this filamentous green algae increased with the increased of the pH of the solution. The experimental adsorption results indicate that the temperature had a negative effect on the amount of methylene blue adsorbed by this biosorbent. The amount of methylene blue adsorbed by the algae decreased with increasing temperature. This phenomenon suggests that physical adsorption is the primary mechanism that controls the adsorption of methylene blue on Ulothrix species.

7. Fungus/fungi as biosorbents

Fungus/fungi have been utilized as the alternative low-cost biosorbents for the removal of dyes from the water environment by a large number of research groups. The capability of fungal biomass in decolorizing of large numbers of dyes has been discussed by Sen et al. (2016). The combination of enzyme degradation and adsorption is the primary mechanism in the decolorization of dyes by fungal biomass (Sen et al., 2016). The ability of the fungus to degrade complex synthetic dyes is mostly due to the availability of extracellular ligninolytic enzymes in the fungus itself. Several of the studies on the utilization of the fungus or fungi to decolorize dyes from the solutions are listed in Table 4.4.

The modification of fungus with chemicals is usually conducted to increase its adsorption capacity. The modification of *Aspergillus versicolor* using CTAB was studied by Huang et al. (2016) to increase its adsorption capability toward Reactive Black 5. The highest removal efficiency of Reactive Black 5 (>98%) by surfactant-modified *A. versicolor* (1.5% CTAB) was achieved at pH 2.0 and contact time of 420 min. The high removal efficiency of surfactant-modified *A. versicolor* is due to the increased active sites of surface functional groups as well as the increased BET surface area. At an acidic pH

TABLE 4.4 Adsorption of dyes using fungus/fungi as biosorbents.

Fungus/fungi	Dye	Parameters	Adsorption capacity, mg/g	Reference
Agaricus bisporus	Reactive Red 2	The fungal was modified by CTAB (cetyl trimethyl ammonium bromide). pH: 2.0—8.0, temperature: 25, 35, 45 °C; contact time: 5—90 min.	141.53	Akar and Divriklioglu (2010)
Aspergillus lentulus FJ172995	Acid Navy Blue, Orange HF, Fast Red A, Acid Sulfone Blue, and Acid Magenta	pH: 4.0—10.0; initial dye concentration: 100—900 mg/L; temperature: 30, 35, 40, 45 °C	212.92	Kaushik and Malik. (2010)
Aspergillus versicolor	Reactive Black 5	The fungal was modified by CTAB; pH: 2.0—8.0; temperature: 30 °C; adsorption time: 0—24 h	227.27	Huang et al. (2016)
Ceriporia lacerata P2	Crystal Violet	pH: 2.0—10.0; initial concentration: 10—500 mg/L; temperature: 20 °C	239.25	Lin et al. (2011)
Coriolopsis sp.	Crystal Violet, Methyl Violet, Cotton Blue, Malachite Green	Initial dye concentration: 50, 100, and 200 mg/L; temperature: 30 °C	n.a	Chen and Ting (2015a)
Cunninghamella elegans	Acid Blue 62, Acid Red 266 and Acid Yellow 49	Contact time: 0—125 min; temperature: 30 °C; pH: 3.0—11.0	1035	Russo et al. (2010)

Continued

TABLE 4.4 Adsorption of dyes using fungus/fungi as biosorbents.—cont'd

Fungus/fungi	Dye	Parameters	Adsorption capacity, mg/g	Reference
Lenzites elegans WDP2	Crystal Violet, Malachite Green, Fuschsin Basic, and Brilliant Green	pH: 7.0; temperature: 30 °C; time: 0—72 h.	n.a	Pandey et al. (2018)
Mucor circinelloides	Congo Red	Temperature: 25, 50, 75 °C; initial concentration of dye: 150, 300, 600, 800, 1000 mg/L	169.49	Azin and Moghimi (2018)
Penicillum restrictum	Reactive Yellow 145	pH: 1—8; temperature: 20, 30, and 40 °C	116.5	Caner et al. (2011)
Rhizopus arrhizus	Methylene blue	Modified with SDS (sodium dodecylsulfate) surfactant. pH: 2—12; SDS concentration: 0—20 mM; temperature: 25 °C; initial concentration of MB: 25—1100 mg/L	1666.6	Aksu et al. (2010)

(2.0), the protonation of several functional groups such as carboxyl, hydroxyl, amide, and amine groups in the surface of surfactant-modified *A. versicolor* occurred. The surface of biosorbent became positively charged, and electrostatic interaction between the surface of biosorbent and negatively charged (SO_3^-) ions of Reactive Black 5 occurred. This phenomenon significantly enhanced the uptake of the anionic dye from the aqueous solution (Huang et al., 2016).

8. Bacteria as biosorbents

As microscale organisms, bacteria also have been widely explored for its potential application as low-cost adsorbents for decolorization of wastewater containing dyes. Several recent studies on the utilization of bacteria as biosorbents for dyes removal from an aqueous environment are summarized in Table 4.5.

The activity and adaptability of bacteria in the wastewater treatment system strongly influence the effectiveness of bacteria in the decolorization process (Meerbergen et al., 2018). Bacteria possess different decolorization mechanisms compared with other conventional biosorbents such as fungus, algae, or other lignocellulosic biomass. In the conventional biosorbents, the removal of color or decolorization process is mainly due to the adsorption process, so basically, the decolorization process using conventional biosorbents will be effective if the concentration of dye in the solution or wastewater is quite low. In the decolorization process using bacteria as the biosorbent, the main decolorization mechanism is degradation rather than adsorption; therefore, this process is likely very effective for wastewater containing a high concentration of dyes (Meerbergen et al., 2018).

9. Equilibrium studies

Various adsorption isotherm equations which were initially developed for the gas-phase adsorption are employed to represent the adsorption equilibria data of various dyes by different kinds of biosorbents. Those equations are either two-parameter models (Langmuir, Freundlich, Dubinin−Radushkevich (DR), Temkin, Flory−Huggins, BET) or three-parameter models (Sips, Toth, and Redlich−Paterson). Among them, Langmuir and Freundlich are the most widely used isotherm equations to represent the adsorption equilibria data due to their simplicity.

Langmuir equation has the form as follows:

$$q_e = q_{\max} \frac{K_L C_e}{1 + K_L C_e} \tag{4.1}$$

Parameters $q_{\max}$ and K_L represent the adsorption capacity of biosorbent toward specific dye pollutants, and K_L is the adsorption affinity. In most cases,

TABLE 4.5 Adsorption of dyes using bacteria as biosorbents.

Bacteria	Dyes	Notes	Reference
Acinetobacter (ST16.16/164)	Reactive Orange 16 and Reactive Green 19	The bacteria were isolated from activated sludge of two wastewater treatment plants located in Flanders, Belgium. The influence of carbon sources, pH, temperature, dye concentration, and concentration of salt addition on the decolorization capability of Acinetobacter was explored. The incubation was conducted for 3 days. The decolorization efficiency of Acinetobacter toward both of azo dyes was > 80%.	Meerbergen et al. (2018)
Klebsiella (ST16.16/ 034)	Reactive Orange 16 and Reactive Green 19	The bacteria were isolated from activated sludge of two wastewater treatment plants located in Flanders, Belgium. The influence of carbon sources, pH, temperature, dye concentration, and concentration of salt addition on the decolorization capability of Klebsiella was explored. The incubation was conducted for 3 days. The decolorization efficiency of Klebsiella toward both of azo dyes was > 80%.	Meerbergen et al. (2018)
Penicillium simplicissimum	Methyl Violet, Crystal Violet, and Cotton Blue	The bacteria were isolated from wastewater at Monash Uni Malaysia. The decolorization process was conducted at 30 °C for 14 days with initial dyes concentration of 50, 100, and 200 mg/L. The removal efficiencies were 98% for Methyl Violet, 95% for Crystal Violet, and 82% for Cotton Blue.	Chen and Ting (2015b)
Pseudomonas aeruginosa	Reactive Red 21, Reactive Orange 16, and Reactive Blue 19	Jack fruit seed powder was employed as cosubstrate. Response Surface Methodology (RSM) was used to evaluate the influence of different process parameters on the decolorization performance of *Pseudomonas aeruginosa*. The bacteria were capable to remove 97.7 ± 0.3 % of Reactive Red 21, 98.9 ± 0.3 % of Reactive Orange 16, and 92.6 ± 0.4 % of Reactive Blue 19.	Mishra et al. (2019)

both of these parameters are temperature dependent. For physical adsorption (exothermic process), the values of parameters q_{max} and K_L decrease with the increase of the temperature of the system. While the opposite behavior is observed for chemical adsorption (endothermic process).

Freundlich adsorption isotherm has the mathematical expression as follows:

$$q_e = K_f C_e^{1/n} \qquad (4.2)$$

The parameters K_f and n represent Freundlich adsorption capacity and heterogeneity of the system, respectively. Usually, the value of parameter n is between 1 and 10. The higher the value of parameter n, the more heterogeneous the adsorption system. Although it does not have the saturation capacity in high concentration and Henry's law at very low concentration, the Freundlich equation could represent the adsorption equilibria data of many systems very well, as indicated in Table 4.6. In all cases, the adsorption experiments were conducted at low to moderate dye concentrations, and at these ranges of concentrations, the drawback of the Freundlich model does not exist; therefore, this adsorption equation could describe the experimental data well (Febrianto et al., 2009).

Another adsorption isotherm model, which was initially developed for the adsorption of gas onto microporous adsorbents, DR equation, also widely employed to correlate the adsorption of dyes onto biosorbents (nonporous materials). The DR equation can be expressed in mathematic form as follows:

$$q_e = q_{max} \exp\left(-\left(\frac{RTln(c_e/c_s)}{\alpha Eo}\right)^2\right) \qquad (4.3)$$

The parameter α is an affinity coefficient that is proportional to the molar volume of the adsorbate. The theoretical value of α can be estimated based on the refractive index of the adsorbate (Ismadji and Bhatia, 2001). Symbol C_s indicates the solubility of the solute in the solvent. The parameter E_o represents solid characteristic energy (usually compared to benzene, which is generally chosen as the reference compound). One of the unique features of the DR equation is in the characteristic curves. If the DR equation could represent the experimental data, all of the adsorption data at different temperatures when plotted as the logarithmic amount adsorbed (q_e) versus the square of potential energy ($RTln(C_e/C_s)$) should lie on the same straight line. However, in all of the studies which were employed, the DR equation failed to provide this characteristic curve, the judgment of the validity of the model to represent the experimental adsorption data is only based on the value of the R^2 (Daneshvar et al., 2012; Ari and Celik, 2013; Lebron et al., 2018; Deniz and

TABLE 4.6 Adsorption equations to represent the equilibria data of the adsorption of dye onto biosorbent.

Biosorbent	Dye	Isotherms used	Isotherm valid	References
Aspergillus niger	Acid Blue 161 and Procion Red MX-5B	Langmuir and Freundlich	Freundlich	Almeida and Corso (2019)
Aspergillus terreus	Acid Blue 161 and Procion Red MX-5B	Langmuir and Freundlich	Freundlich	Almeida and Corso (2019)
Aspergillus versicolor	Reactive black 5	Langmuir and Freundlich	Langmuir	Huang et al. (2016)
Banana trunk—activated carbon	Methylene blue	Langmuir, Freundlich, DR, Temkin, Frumkin, Harkins-Jura, and Smith	Freundlich	Danish et al. (2018)
Carpinus betulus sawdust	Basic red 46	Langmuir, Freundlich, and DR	Freundlich and Langmuir	Deniz and Yildis (2019)
Cashew nutshell—based carbons	Methylene blue	Langmuir and Freundlich	Freundlich and Langmuir	Spagnoli et al. (2017)
Ceriporia lacerata P2	Crystal violet	Langmuir, Freundlich, Koble-Corrigan, and Scatchard	Koble-Corrigan	Lin et al. (2011)
Chlorella pyrenoidosa	Methylene blue	Langmuir, Freundlich, DR, Temkin	Langmuir	Lebron et al. (2018)
	Direct Red-31	Langmuir and Freundlich	Langmuir and Freundlich	Sinha et al. (2016)
Chlorella vulgaris	Supranol Red 3BW	Langmuir and Freundlich	Langmuir and Freundlich	Lim et al. (2010)
Corn silk	Reactive Blue 19, and Reactive Red 218	Langmuir, Freundlich, DR, Temkin, Halsey, and Harkins-Jura	Freundlich and Temkin	Degermenci et al. (2019)

Date palm	Methylene blue	Langmuir, Freundlich, and DR	Freundlich	Esmaeili and Foroutan (2019)
Eucalyptus	Methylene blue	Langmuir, Freundlich, and DR	Freundlich	Esmaeili and Foroutan (2019)
Furfural lignocellulosic waste	Methyl Orange and Rhodamine B	Langmuir and Freundlich	Langmuir (Methyl orange), and Freundlich (Rhodamine B)	Chen et al. (2019)
Kefir grains	Remazol navy	Langmuir, Freundlich, and Temkin	Temkin and Langmuir	Erdoğdular and Apar (2019)
Laminaria japonica	Methylene blue	Langmuir and Sips	Langmuir	Shao et al. (2017)
Macroalga Stoechospermum marginatum	Acid Blue 25, Acid Orange 7, Acid Black 1	Langmuir, Freundlich, DR, and Temkin	Freundlich	Daneshvar et al. (2012)
Microalgae Scenedesmus	Methylene blue	Langmuir	Langmuir	Afshariani and Roosta (2019)
Mucor circinelloides	Congo red	Langmuir and Freundlich	Freundlich	Azin and Moghimi (2018)
Neonectria radicicola	Acid Orange 51, Reactive Red 75, and Direct Blue 86	Langmuir, Freundlich, Redlich−Peterson, Toth, and Temkin	Freundlich and Temkin	Ghariani et al. (2019)

TABLE 4.6 Adsorption equations to represent the equilibria data of the adsorption of dye onto biosorbent.—cont'd

Biosorbent	Dye	Isotherms used	Isotherm valid	References
Neurospora sitophila cells—Zeamays silk tissue biomass system	Reactive blue 49	Langmuir and Freundlich	Langmuir	Akar and Celik (2011)
Olive stone by-product	Alizarin red and methylene blue	Langmuir, Freundlich, Redlich−Peterson, and Temkin	Redlich−Peterson	Albadarin and Mangwandi (2015)
Pomegranate peel	Malachite green	Langmuir, Freundlich, Temkin, DR, and Redlich−Peterson	Langmuir	Gunduz and Bayrak (2017)
Prunus dulcis leaves	Acid Blue 113	Langmuir and Freundlich	Langmuir	Jain and Gogate (2019)
Pyracantha coccinea	Orange G	Langmuir, Freundlich, DR	Langmuir	Ari and Celik (2013)
Rhizopus oligosporus	Acid Blue 161 and Procion Red MX-5B	Langmuir and Freundlich	Freundlich	Almeida and Corso (2019)
Saccharomyces cerevisiae	Brilliant green and methylene blue	Langmuir and Freundlich	Freundlich	Ghaedi et al. (2013)
Sargassum dentifolium	Methylene blue	Langmuir and Freundlich	Freundlich	Moghazy et al. (2019)

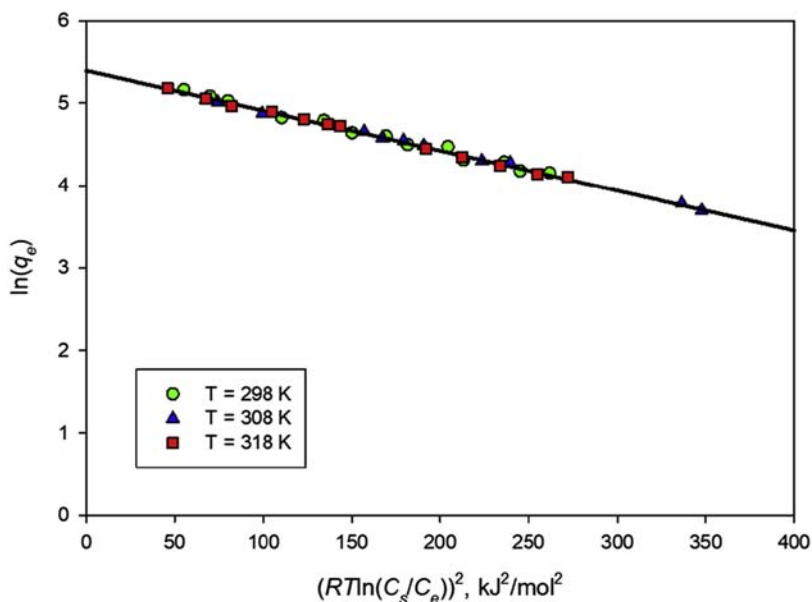|				
Sargassum muticum	Methylene blue	Langmuir, Freundlich, DR, Temkin	DR and Temkin	El Atouani et al. (2019)
Sesame hull	Methylene blue	Langmuir, Freundlich, and Temkin	Langmuir	Feng et al. (2011)
Sesame straw	Methylene blue	Langmuir and Freundlich	Langmuir	Feng et al. (2017)
Sour lemon sawdust	Methylene blue	Langmuir, Freundlich, and DR	Freundlich	Esmaeili and Foroutan (2019)
soybean hulls	Reactive Red 195	Langmuir, Freundlich, Toth, Sips, Radke—Praustnitz, Temkin, and BET	Langmuir, BET, and Toth	Módenes et al. (2019)
Spirulina maxima	Methylene blue	Langmuir, Freundlich, DR, Temkin	Freundlich and Temkin	Lebron et al. (2018)
Swede rape straw	Methylene blue	Langmuir, Freundlich, and Temkin	Langmuir	Feng et al. (2013)
Trichoderma harzianum	Reactive black B	Langmuir, Freundlich, and Temkin	Freundlich	Karthik et al. (2019)
Ulva fasciata	Methylene blue	Langmuir and Freundlich	Freundlich	Moghazy et al. (2019)
Walnut shell	Malachite green	Langmuir, Temkin, Freundlich, and Dubinin—Kaganer—Radushkevich (DKR)	Langmuir	Hajialigol and Masoum (2019)
Walnut shell	Methyl blue and Congo Red	Langmuir	Langmuir	Liu et al. (2019)
Water hyacinth	Amaranth anionic dye	Langmuir, Freundlich, Temkin, Halsey, DR, Sips, Redlich—Peterson, Radke-Prausnitz, Toth	Langmuir, Sips, Redlich—Petersen	Guerrero-Coronilla et al. (2015)

FIG. 4.2 The characteristic curve of the adsorption of methyl violet onto jackfruit peel waste activated carbon.

Yildis, 2019; Degermenci et al., 2019; El Atouani et al., 2019; Esmaeili and Foroutan, 2019). The characteristic curve of the adsorption of methyl violet onto jackfruit peel waste-activated carbon is given in Fig. 4.2.

Based on Fig. 4.2, it is evident that the DR equation can represent the equilibria data of the adsorption of methyl violet onto jackfruit peel waste−activated carbon well. As mentioned previously that the DR equation was developed for the adsorption of gas onto porous solids, therefore, this model is mostly applicable to represent the adsorption equilibria data of various substances onto porous materials such as activated carbons.

Temkin equation is also a popular model to represent the adsorption of dyes onto various biomass systems. Similar to the previous adsorption isotherm models, the Temkin model was also developed for the gas-phase adsorption (adsorption of H_2 onto Pt electrodes). The mathematic expression of Temkin equation is as follows:

$$q_e = \frac{RT}{b_T} ln(K_T C_e) \qquad (4.4)$$

The parameter b_T represents the heat of adsorption, while the binding energy of the adsorption at equilibrium condition is given by symbol K_T. Temkin equation is also frequently used by many researchers to correlate the

biosorption of dyes onto biosorbents such as adsorption of methylene blue on banana trunk−activated carbon (Danish et al., 2018), adsorption of methylene blue on *Chlorella pyrenoidosa* (Lebron et al., 2018), adsorption of acid dyes onto brown macroalgae *Stoechospermum marginatum* (Daneshvar et al., 2012), adsorption of Reactive Blue 19, and Reactive Red 218 on corn silk (Degermenci et al., 2019), adsorption of Remazol navy on kefir grains (Erdoğdular and Apar, 2019), adsorption of Acid Orange 51, Reactive Red 75, and Direct Blue 86 on Neonectria radicicola (Ghariani et al., 2019), etc. In several systems, this equation gave better performance than other adsorption equations in correlating the experimental adsorption data of dyes onto biosorbents (Lebron et al., 2018; Degermenci et al., 2019; El Atouani et al., 2019; Ghariani et al., 2019). In general, the adsorption of dyes onto biosorbents involvs very complex phenomena; several factors such as the pH of the solution, solubility of dyes in water, and the surface chemistry of the biosorbents play crucial roles on the uptake of dye molecules by biosorbents. Since the development of the Temkin adsorption equation is only based on straightforward assumptions, the complex phenomena of dyes adsorption by the biosorbents cannot be captured by this equation, and therefore, in most cases, this equation fails to represent the adsorption equilibria data.

Compared with the other two parameter adsorption equations, the Halsey isotherm is seldom used to represent the equilibrium data of the adsorption of dyes onto biosorbents. Halsey isotherm was derived according to the condensation of gases in a multilayer condition (the distance relatively far from the surface of the solid). The Halsey isotherm equation can be written as follows:

$$q_e = \left(\frac{K_H}{C_e}\right)^{1/n_H} \tag{4.5}$$

where K_H and n_H are the parameters of the Halsey isotherm equation. This equation fails to represent the adsorption of Amaranth anionic dye onto water hyacinth (Guerrero-Coronilla et al., 2015).

Similar to Halsey isotherm equation, the BET isotherm is also rarely employed to correlate the adsorption data of dyes onto biosorbents. The BET model for liquid-phase adsorption has the form as follows:

$$q_e = q_{max}\frac{BC_e}{(C_e - C_s^*)[1 + (B - 1)(C_e/C_s)]} \tag{4.6}$$

The development of the BET model used a similar kinetic concept of Langmuir isotherm (rate of adsorption = rate of desorption). Unlike the Langmuir equation, the restriction that one adsorption site can be occupied by one molecule of adsorbate has been omitted in the BET model. The BET model has been successfully employed to correlate the adsorption data of Reactive Red 195 on the soybean hull (Módenes et al., 2019).

In several cases, the available two-parameter adsorption equations could not represent the adsorption equilibria data well, and for this reason, three-parameter adsorption isotherms were developed. Sips isotherm is the three-parameter model which was developed to overcome the drawback of the Freundlich equation; this equation possesses saturation capacity at relatively high concentration of the adsorbate.

$$q_e = q_{\max}\frac{(K_s C_e)^n}{1 + (K_s C_e)^n} \tag{4.7}$$

Similar to Freundlich, the parameter n in the Sips equation also represents the heterogeneity of the adsorption system. For the homogeneous system, the parameter n in Sips equation is close to unity, and it will become the Langmuir equation.

As a three-parameter equation, the Sips equation is more superior in representing the adsorption equilibria than other two-parameter equations. Sips equation could represent the adsorption equilibria for many systems such as water hyacinth—Amaranth anionic dye (Guerrero-Coronilla et al., 2015), acid-treated coffee husk—Malachite Green (Murthy et al., 2019), *Eugenia umbelliflora* Berg—Methylene Blue (Postai and Rodrigues, 2018), *Anethum graveolens*—Methylene Blue (Hamitouche et al., 2017), Beechwood—Direct Red (Muntean et al., 2017), etc. Since the Sips equation also does not have a correct Henry's law at very low concentration, therefore, this equation mostly fails to represent the adsorption data at low concentration.

Toth equation is another empirical three-parameter adsorption isotherm, this equation is able to represent many adsorption equilibria of heterogeneous systems.

$$q_e = q_{\max}\frac{K_T C_e}{\left(1 + (K_T C_e)^n\right)^{1/n}} \tag{4.8}$$

Toth equation has a correct Henry law for very low concentration. Being an empirical three-parameter equation, Toth should be able to describe the experimental data for most complex adsorption systems. However, this equation failed to represent the adsorption equilibria of particular systems such as water hyacinth—Amaranth anionic dye (Guerrero-Coronilla et al., 2015), Neonectria radicicola—Acid Orange 51, Neonectria radicicola—Reactive Red 75, and Neonectria radicicola—Direct Blue 86 (Ghariani et al., 2019). While for the biosorption Reactive Red 195 onto soybean hull, Toth gave the best correlation compared with other available isotherm equations (Módenes et al., 2019).

Table 4.6 indicates that Redlich—Paterson isotherm is also a popular model to represent the equilibria data of the adsorption of dyes on biosorbents. The Redlich—Paterson isotherm has the form as follows:

$$q_e = \frac{K_R C_e}{1 + a_R C_e^\beta} \tag{4.9}$$

For several adsorption systems, the Redlich−Paterson could fit the experimental data well, as indicated in Table 4.6. Eq. (4.9) combines both characteristics of Freundlich and Langmuir equations. When β is equal to 0, Eq. (4.9) reduces to Henry's law form, and if β is equal to 1, it becomes a Langmuir equation.

10. Kinetic studies

For the design of efficient and effective adsorption system, both equilibria and kinetic data are required. Many kinetic models are available to represent the adsorption kinetic of dyes onto biosorbents. The most widely used models to describe the kinetics of adsorption of dyes onto biosorbents are pseudo−first-order and pseudo−second-order equations. Both of those equations were developed according to the concept of chemical reaction that occurs on the surface of adsorbent (Plazinski et al., 2009).

In 1898, Lagergren proposed the pseudo−first-order equation. This empirical equation was developed to describe the adsorption of malonic and ocalic acids on the surface of the charcoal (Plazinski et al., 2009). The pseudo−first-order equation has the following mathematical form:

$$q_t = q_e(1 - \exp(k_1 t)) \tag{4.10}$$

where q_t is the amount of dye adsorbed by biosorbent at time t, while q_e and k_1 are the parameters of the pseudo−first order which indicate the amount adsorbed at equilibrium condition and time scaling factor. The parameters q_e and k_1 are usually obtained through the linear regression method. Since k_1 is a time scaling factor, the higher the value of this parameter, the sooner the system reaches equilibrium (shorter time required) as illustrated in Fig. 4.3.

Usually, the parameter k_1 is dependent on the pH of the solution, temperature, as well as the initial concentration of the solute (Albadarin and Mangwandi, 2015; Akar and Celik, 2011; Akar and Divriklioglu, 2010).

Pseudo−second-order equation was proposed by Blanchard et al. (1984), which has the form as follows:

$$q_t = \frac{q_e^2 k_2 t}{1 + q_e k_2 t} \tag{4.11}$$

Similar to the parameter k_1 in pseudo−first order, the parameter k_2 is also a time scaling factor. The effect of k_2 on fractional loading of dye on biosorbent is depicted in Fig. 4.4.

The higher the value of k_2, the shorter the time required by the system to reach the equilibrium condition. Similar to k_1, k_2 is also influenced by the adsorption condition such as initial concentration, pH of the solution, and temperature. In most adsorption systems, the pseudo−second order gave better
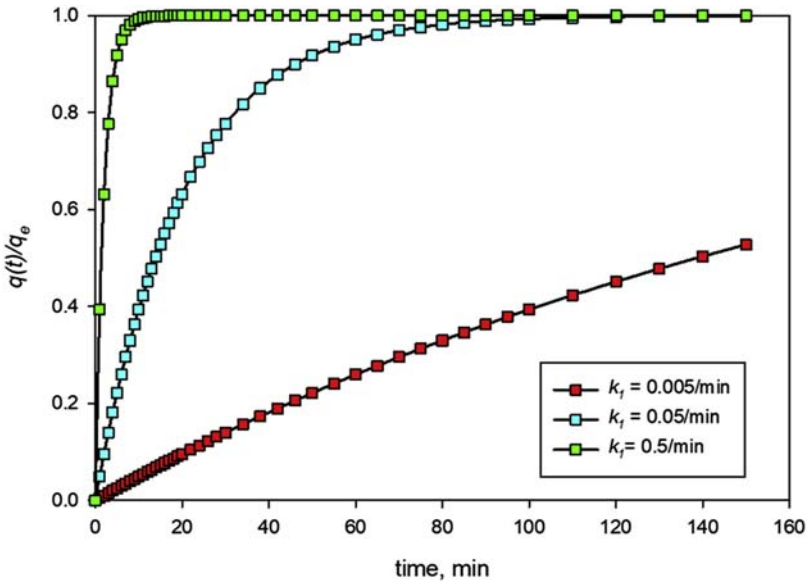
FIG. 4.3   The effect of k_1 on fractional loading of dye on biosorbent.
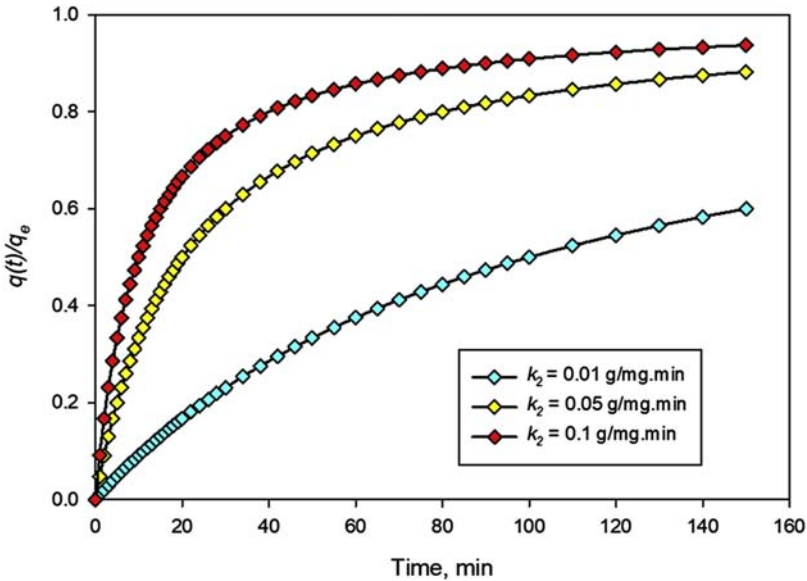

FIG. 4.4   The effect of k_2 on fractional loading of dye on biosorbent.

representation of the experimental data compared with the pseudo−first order (Da Silva et al., 2019; Liu et al., 2019; Módenes et al., 2019; Moghazy et al., 2019; Rehman et al., 2019; Lebron et al., 2018; Huang et al., 2016; Ghaedi et al., 2013). The parameter q_e in pseudo−second order equation is less sensitive from the effect of the random experimental error (Plazinski et al., 2009); therefore, this equation gives better prediction than the pseudo−first-order equation.

11. Thermodynamic of adsorption of dyes on biosorbents

The thermodynamic of adsorption is also one of the important information which is required for the design of the adsorption systems. Unfortunately, there is no single equipment that can be used to determine the thermodynamics of adsorption directly. The only option to obtain the thermodynamic of adsorption is through the interpretation of the adsorption isotherms using Van't Hoff equation

$$lnK_D = \frac{\Delta S^o}{R} - \frac{\Delta H^o}{RT} \tag{4.12}$$

where K_D is the linear sorption distribution coefficient, ΔS^o and ΔH^o are the standards of entropy and enthalpy change, respectively. In most cases, the value of K_D was obtained through a simple relation $K_D = q_e/C_e$ which is not a correct one (Da Silva et al., 2019; Degermenci et al., 2019; Deniz and Yildiz, 2019; Danish et al., 2018; Daneshvar et al., 2012; Akar and Celic, 2011; Caner et al., 2011; Akar and Divriklioglu, 2010). Through this simple relation, in one adsorption isotherm, there are many q_e and C_e, and any single relation between q_e and C_e will produce one value of K_D, and it is not clear which value of K_D should be chosen. The value of K_D should be calculated based on the method of Khan and Singh (1987). Through a straight-line plot of $ln(q_e/c_e)$ versus C_e, the value of K_D will be obtained (see Fig. 4.5). Through Van't Hoff equation, the value of the standard of entropy and enthalpy change can be obtained.

Another valuable thermodynamic property of adsorption is Gibb's free energy change (ΔG^o) which can be calculated through the following relation:

$$\Delta G^o = -RTlnK_D \tag{4.13}$$

If the value of ΔG^o is negative, it means that the adsorption process is spontaneous and feasible in the term of thermodynamic (Daneshvar et al., 2012; Akar and Celic, 2011; Caner et al., 2011; Aksakal and Ucun, 2010; Brito et al., 2010). The positive value of ΔG^o indicates the adsorption of dyes onto the surface of biosorbents is not a spontaneous process; the thermodynamic equilibrium condition between adsorption and desorption processes could not be achieved (Degermenci et al., 2019; Guerrero-Coronilla et al., 2015).

The exothermicity and endothermicity of the adsorption process can be determined from the value of ΔH^o. If the uptake of adsorbate by adsorbent
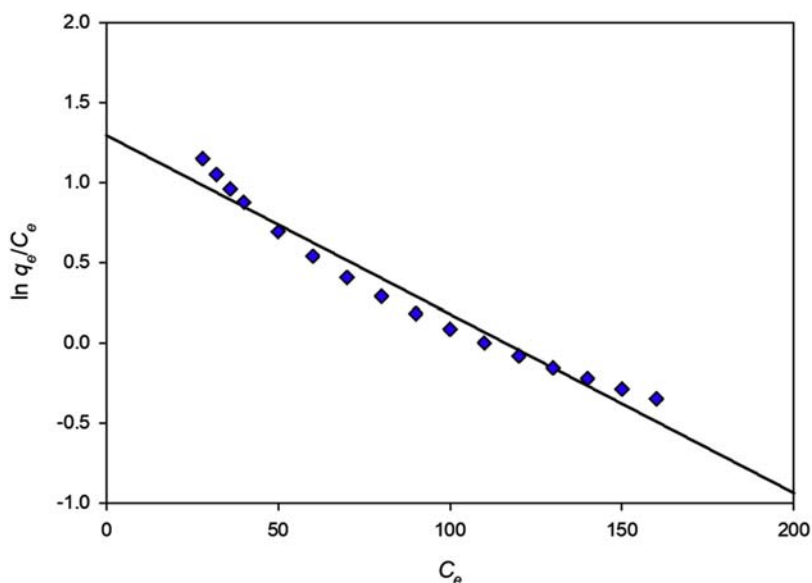
FIG. 4.5 Plot for determination of the value of K_D.

increases with temperature, the adsorption process is endothermic which is indicated by the positive value of ΔH^o (Degermenci et al., 2019; Guerrero-Coronilla et al., 2015; Daneshvar et al., 2012; Akar and Celic, 2011; Aksakal and Ucun, 2010). While the negative value of ΔH^o suggests that the adsorption process is exothermic, in this case, the temperature has a negative influence on the amount adsorbed by the adsorbent (Brito et al., 2010).

The randomness of the adsorption system is measured by ΔS^o. Positive value of ΔS^o indicates that adsorbate molecules possess a high affinity toward the active sites of the adsorbent. The adsorption system becomes more random between both interfaces of solute and adsorbent as the entropy of the system increases (Degermenci et al., 2019; Daneshvar et al., 2012; Akar and Celic, 2011; Aksakal and Ucun, 2010). When the values of ΔS^o is negative, the adsorption systems become more order (Guerrero-Coronilla et al., 2015; Brito et al., 2010).

12. Conclusions

Various low-cost biosorbents have explored its potential application as industrial adsorbents for the removal of dyes from aqueous solutions or wastewater. The performance of the biosorbents in removing dyes is strongly influenced by the pH and temperatures of the solution. Among various adsorption isotherm equations employed to correlate the experimental data, Langmuir and Freundlich could represent most of the adsorption systems very

well. For kinetic models, the pseudo—second order is the best choice to represent the adsorption kinetic data. The thermodynamic of adsorption was obtained through the interpretation of the adsorption isotherms using Van't Hoff equation. From the results of the studies, it seems the utilization of these low-cost biosorbents in industrial scale is still far from reality.

References

Afroze, S., Sen, T.K., 2018. A review on heavy metal ions and dye adsorption from water by agricultural solid waste adsorbents. Water Air Soil Pollut. 229, 225.

Afshariani, F., Roosta, A., 2019. Experimental study and mathematical modeling of biosorption of methylene blue from aqueous solution in a packed bed of microalgae Scenedesmus. J. Clean. Prod. 225, 133—142.

Akar, T., Celik, S., 2011. Efficient biosorption of a reactive dye from contaminated media by Neurospora sitophila cells — zeamays silk tissue biomass system. J. Chem. Technol. Biotechnol. 86, 1332—1341.

Akar, T., Divriklioglu, M., 2010. Biosorption applications of modified fungal biomass for decolorization of Reactive Red 2 contaminated solutions: batch and dynamic flow mode studies. Bioresour. Technol. 101, 7271—7277.

Aksakal, O., Ucun, H., 2010. Equilibrium, kinetic and thermodynamic studies of the biosorption of textile dye (Reactive Red 195) onto Pinus sylvestris L. J. Hazard Mater. 181, 666—672.

Aksu, Z., Ertugrul, S., Donmez, G., 2010. Methylene Blue biosorption by Rhizopus arrhizus: effect of SDS (sodium dodecylsulfate) surfactant on biosorption properties. Chem. Eng. J. 158, 474—481.

Albadarin, A.B., Mangwandi, C., 2015. Mechanisms of alizarin red s and methylene blue biosorption onto olive stone by-product: isotherm study in single and binary systems. J. Environ. Manag. 164, 86—93.

Almeida, E.J.R., Corso, C.R., 2019. Decolorization and removal of toxicity of textile azo dyes using fungal biomass pelletized. Int. J. Environ. Sci. Technol. 16, 1319—1328.

Anastopoulos, I., Bhatnagar, A., Hameed, B.H., Ok, Y.S., Omirou, M., 2017. A review on waste-derived adsorbents from sugar industry for pollutant removal in water and wastewater. J. Mol. Liq. 240, 179—188.

Anastopoulos, I., Kyzas, G.Z., 2014. Agricultural peels for dye adsorption: a review of recent literature. J. Mol. Liq. 200, 381—389.

Ari, A.G., Celik, S., 2013. Biosorption potential of Orange G dye by modified Pyracantha coccinea: batch and dynamic flow system applications. Chem. Eng. J. 226, 263—270.

Astuti, W., Sulistyaningsih, T., Kusumastuti, E., Ratna, G.Y., Thomas, S., Kusnandi, R.Y., 2019. Thermal conversion of pineapple crown leaf waste to magnetized activated carbon for dye removal. Bioresour. Technol. 287, 121426.

Azin, E., Moghimi, H., 2018. Efficient mycosorption of anionic azo dyes by Mucor circinelloides: surface functional groups and removal mechanism study. J. Environ. Chem. Eng. 6, 4114—4123.

Baytar, O., Sahin, O., Saka, C., 2018. Sequential application of microwave and conventional heating methods for the preparation of activated carbon from biomass and its methylene blue adsorption. Appl. Therm. Eng. 138, 542—551.

Bhatnagar, A., Sillapaa, M., Witek-Krowiak, A., 2015. Agricultural waste peels as versatile biomass for water purification — a review. Chem. Eng. J. 270, 244—271.

Bhatnagar, A., Vilar, V.J.P., Botelho, C.M.S., Boanventura, R.A.R., 2010. Coconut-based bio-sorbents for water treatment—a review of the recent literature. Adv. Colloid Interface Sci. 160, 1–15.

Bhomic, P.C., Baruah, A.S.M., Pongener, C., Sinha, D., 2018. Activated biocarbon for adsorption of anionic dye from aqueous solution: isotherm, kinetic, thermodynamic and regeneration studies. Sust. Chem. Pharm. 10, 41–49.

Blanchard, G., Maunaye, M., Martin, G., 1984. Removal of heavy metals from waters by means of natural zeolites. Water Res. 18, 1501–1507.

Brito, S.M.D.O., Andrade, H.M.C., Soares, L.F., de Azevedo, R.P., 2010. Brazil nutshells as new biosorbent to remove methylene blue and indigo carmine from aqueous solutions. J. Hazard Mater. 174, 84–92.

Caner, M., Kiran, I., Ilhan, S., Pinarbasi, A., Iscen, C.F., 2011. Biosorption of reactive yellow 145 dye by dried penicillum restrictum: isotherm, kinetic, and thermodynamic studies. Separ. Sci. Technol. 46, 2283–2290.

Celekli, A., Al-Nuaimi, A.S., Bozkurt, H., 2019. Adsorption kinetics and isotherms of reactive red 120 on Moringa oleifera seed as an eco-friendly process. J. Mol. Struct. 1195, 168–178.

Chen, S.H., Ting, A.S.Y., 2015a. Biodecolorization and biodegradation potential of recalcitrant triphenylmethane dyes by *Coriolopsis* sp. isolated from compost. J. Environ. Manag. 150, 274–280.

Chen, S.H., Ting, A.S.Y., 2015b. Biosorption and biodegradation potential of triphenylmethane dyes by newly discovered Penicillium simplicissimum isolated from indoor wastewater sample. Int. Biodeterior. Biodegrad. 103, 1–7.

Chen, X., Li, H., Liu, W., Zhang, X., Wu, Z., Bi, S., Zhang, W., 2019. Effective removal of methyl orange and rhodamine B from aqueous solution using furfural industrial processing waste: furfural residue as an eco-friendly biosorbent. Colloids Surf., A 583, 123976.

Daneshvar, E., Kousha, M., Sohrabi, M.S., Khataee, A., Converti, A., 2012. Biosorption of three acid dyes by the brown macroalga Stoechospermum marginatum: isotherm, kinetic and thermodynamic studies. Chem. Eng. J. 195–196, 297–306.

Danish, M., Ahmad, T., Majeed, S., Ahmad, M., Ziyang, L., Pin, Z., Iqubal, S.M.S., 2018. Use of banana trunk waste as activated carbon in scavenging methylene blue dye: kinetic, thermo-dynamic, and isotherm studies. Biores. Technol. Rep. 3, 127–137.

Da Rosa, A.L.D., Carissimi, E., Dotto, G.L., Sander, H., Feris, L.A., 2018. Biosorption of rhodamine B dye from dyeing stones effluents using the green microalgae Chlorella pyr-enoidosa. J. Clean. Prod. 198, 1302–1310.

Da Silva, D.C.C., Pietrobelli, J.M.T.A., 2019. Residual biomass of chia seeds (Salvia hispanica) oil extraction as low cost and eco-friendly biosorbent for effective reactive yellow B2R textile dye removal: characterization, kinetic, thermodynamic and isotherm studies. J. Environ. Chem. Eng. 7, 1038000.

Degermenci, G.D., Degermenci, N., Ayvaoglu, V., Durmaz, E., Cakir, D., Akan, E., 2019. Adsorption of reactive dyes on lignocellulosic waste; characterization, equilibrium, kinetic and thermodynamic studies. J. Clean. Prod. 225, 1220–1229.

Deniz, F., Karaman, S., 2011. Removal of Basic Red 46 dye from aqueous solution by pine tree leaves. Chem. Eng. J. 170, 67–74.

Deniz, F., Saygideger, S.D., 2010. Equilibrium, kinetic and thermodynamic studies of Acid Orange 52 dye biosorption by Paulownia tomentosa Steud. leaf powder as a low-cost natural bio-sorbent. Bioresour. Technol. 101, 5137–5143.

Deniz, F., Saygideger, S.D., 2011. Removal of a hazardous azo dye (Basic Red 46) from aqueous solution by princess tree leaf. Desalination 268, 6–11.

Deniz, F., Yildiz, H., 2019. Bioremediation potential of a widespread industrial biowaste as renewable and sustainable biosorbent for synthetic dye pollution. Int. J. Phytoremediation 21, 259−267.

Dogar, C., Gurses, A., Acıkyıldız, M., Ozkan, E., 2010. Thermodynamics and kinetic studies of biosorption of a basic dye from aqueous solution using green algae Ulothrix sp. Colloids Surf. B Biointerfaces 76, 279−285.

Dos Santos, K.J.L., dos Santos, G.E.D.S., de Sa, I.M.G.L., Ide, A.H., Duarte, J.L.D.S., Carvalho, S.H.V.D., Soletti, J.I., Meili, L., 2019. Wodyetia bifurcata biochar for methylene blue removal from the aqueous matrix. Bioresour. Technol. 293, 122093.

Du, C., Yang, H., Wu, Z., Ge, X., Cravotto, G., Ye, B.C., Kaleem, I., 2016. Microwave-assisted preparation of almond shell-based activated carbon for methylene blue adsorption. Green Process. Synth. 5, 395−406.

El Atouani, S., Belattmania, Z., Reani, A., Tahiri, S., Aarfane, A., Bentiss, F., Jama, C., Zrid, R., Sabour, B., 2019. Brown seaweed sargassum muticum as low-cost biosorbent of methylene blue. Int. J. Environ. Res. 13, 131−142.

Emrooz, H.B.M., Maleki, M., Shokouhimehr, M., 2019. Excellent adsorption of orange acid II on a water fern− derived micro- and mesoporous carbon. J. Taiwan Inst. Chem. Eng. 102, 99−109.

Erdoğdular, A.O., Apar, D.K., 2019. Bioremoval of reactive dye Remazol Navy by kefir grains. Appl. Biol. Chem. 62, 22.

Esmaeili, H., Foroutan, R., 2019. Adsorptive behavior of methylene blue onto sawdust of sour lemon, date palm, and Eucalyptus as agricultural wastes. J. Dispersion Sci. Technol. 40, 990−999.

Febrianto, J., Kosasih, A.N., Sunarso, J., Ju, Y.H., Indraswati, N., Ismadji, S., 2009. Equilibrium and kinetic studies in adsorption of heavy metals using biosorbent: a summary of recent studies. J. Hazard Mater. 162, 616−645.

Feng, Y., Yang, F., Wang, Y., Ma, L., Wu, Y., Kerr, P.G., Yang, L., 2011. Basic dye adsorption onto an agro-based waste material − sesame hull (Sesamum indicum L.). Bioresour. Technol. 102, 10280−10285.

Feng, Y., Dionysiou, D.D., Wu, Y., Zhou, H., Xue, L., He, S., Yang, L., 2013. Adsorption of dyestuff from aqueous solutions through oxalic acid-modified swede rape straw: adsorption process and disposal methodology of depleted bioadsorbents. Bioresour. Technol. 138, 191−197.

Feng, Y., Liu, Y., Xue, L., Sun, H., Guo, Z., Zhang, Y., Yang, L., 2017. Carboxylic acid functionalized sesame straw: a sustainable cost-effective bioadsorbent with superior dye adsorption capacity. Bioresour. Technol. 238, 675−683.

Fiorentin, L.D., Trigueros, D.E.G., Modenes, A.N., Espinoza-Quinones, F.R., Pereira, N.C., Barros, S.T.D., Santos, O.A.A., 2010. Biosorption of reactive blue 5G dye onto drying orange bagasse in batch system: kinetic and equilibrium modeling. Chem. Eng. J. 163, 68−77.

Ghaedi, M., Hajati, S., Barazesh, B., Karimi, F., Ghezelbash, G., 2013. Saccharomyces cerevisiae for the biosorption of basic dyes from binary component systems and the high order derivative spectrophotometric method for simultaneous analysis of Brilliant green and Methylene blue. J. Ind. Eng. Chem. 19, 227−233.

Ghariani, B., Hadrich, B., Louati, I., Mtibaa, R., Daassi, D., Rodriguez-Couto, S., Nasri, M., Mechichi, T., 2019. Porous heat-treated fungal biomass: preparation, characterization and application for removal of textile dyes from aqueous solutions. J. Porous Mater. 26, 1475−1488.

Gregory, P., 1990. Classification of Dyes by Chemical Structure. The Chemistry and Application of Dyes. Plenum Press, New York.

Guerrero-Coronilla, I., Morales-Barrera, L., Cristiani-Urbina, E., 2015. Kinetic, isotherm and thermodynamic studies of amaranth dye biosorption from aqueous solution onto water hyacinth leaves. J. Environ. Manag. 152, 99−108.

Gunduz, F., Bayrak, B., 2017. Biosorption of malachite green from an aqueous solution using pomegranate peel: equilibrium modelling, kinetic and thermodynamic studies. J. Mol. Liq. 243, 790−798.

Guo, F., Li, X., Jiang, X., Zhao, C., Rao, Z., 2018. Characteristics and toxic dye adsorption of magnetic activated carbon prepared from biomass waste by modified one-step synthesis. Colloid. Surface. Physicochem. Eng. Aspect. 555, 43−54.

Gupta, K., Khatri, O.P., 2019. Fast and efficient adsorptive removal of organic dyes and active pharmaceutical ingredient by microporous carbon: effect of molecular size and charge. Chem. Eng. J. 378, 122218.

Hajialigol, S., Masoum, S., 2019. Optimization of biosorption potential of nano biomass derived from walnut shell for the removal of Malachite Green from liquids solution: experimental design approaches. J. Mol. Liq. 286, 110904.

Hamitouche, A., Haffas, M., Boudjemaa, A., Benammar, S., Sehailia, M., Bachari, K., 2017. Efficient biosorption of methylene blue, malachite green and methyl violet organic pollutants on biomass derived from Anethum graveolens: an eco-benign approach for wastewater treatment. Desalin. Water Treat. 75, 225−236.

Huang, J., Liu, D., Lu, J., Wang, H., Wei, X., Liu, J., 2016. Biosorption of reactive black 5 by modified Aspergillus versicolor biomass: kinetics, capacity and mechanism studies. Colloid. Surface. Physicochem. Eng. Aspect. 492, 242−248.

Ismadji, S., Bhatia, S.K., 2001. Characterization of activated carbons using liquid-phase adsorption. Carbon 39, 1237−1250.

Jain, S.N., Gogate, P.R., 2019. Adsorptive removal of azo dye in a continuous column operation using biosorbent based on NaOH and surfactant activation of Prunus dulcis leaves. Desalin. Water Treat. 141, 331−341.

Javed, F., Feroze, N., Ikhlaq, A., Kazmi, M., Ahmad, S.W., Munir, H.M.S., 2019. Biosorption potential of Sapindus mukorossi dead leaves as a novel biosorbent for the treatment of Reactive Red 241 in aqueous solution. Desalin. Water Treat. 137, 345−357.

Karthik, V., Sivarajasekar, N., Padmanaban, V.C., Nakkeeran, E., Selvaraju, N., 2019. Biosorption of xenobiotic Reactive Black B onto metabolically inactive T. harzianum biomass: optimization and equilibrium studies. Int. J. Environ. Sci. Technol. 16, 3625−3636.

Kaushik, P., Malik, A., 2010. Alkali, thermo and halo tolerant fungal isolate for the removal of textile dyes. Colloids Surf. B Biointerfaces 81, 321−328.

Khan, A.A., Singh, R.P., 1987. Adsorption thermodynamics of carbofuran on Sn(IV) arsenosillicate in H$^+$, Na$^+$ and Ca$^+$ forms. Colloid. Surface. 24, 33−42.

Lebron, Y.A.R., Moreira, V.R., Santos, L.V.S., Jacob, R.S., 2018. Remediation of methylene blue from aqueous solution by Chlorella pyrenoidosa and Spirulina maxima biosorption: equilibrium, kinetics, thermodynamics and optimization studies. J. Environ. Chem. Eng. 6, 6680−6690.

Lebron, Y.A.R., Moreira, V.R., Santos, L.V.S., 2019. Studies on dye biosorption enhancement by chemically modified Fucus vesiculosus, Spirulina maxima and Chlorella pyrenoidosa algae. J. Clean. Prod. 240, 118197.

Lim, S.L., Chu, W.L., Phang, S.M., 2010. Use of Chlorella vulgaris for bioremediation of textile wastewater. Bioresour. Technol. 101, 7314−7322.

Lesmana, S.O., Febriana, N., Soetaredjo, F.E., Sunarso, J., Ismadji, S., 2009. Studies on potential applications of biomass for the separation of heavy metals from water and wastewater. Biochem. Eng. J. 44, 19−41.

Lin, Y., He, X., Han, G., Tian, Q., Hu, W., 2011. Removal of Crystal Violet from aqueous solution using powdered mycelial biomass of Ceriporia lacerata P2. J. Environ. Sci. 23, 2055−2062.

Liu, M., Li, X., Du, Y., Han, R., 2019. Adsorption of methyl blue from solution using walnut shell and reuse in secondary adsorption for Congo red. Bioreso. Technol. Rep. 5, 238−242.

Mahmoodi, N.M., Hayati, B., Bahrami, H., Arami, M., 2011. Dye adsorption and desorption properties of mentha pulegium in single and binary systems. J. Appl. Polym. Sci. 122, 1489−1499.

Mamani, A., Ramirez, N., Deiana, C., Gimenez, M., Sardella, F., 2019. Highly microporous sorbents from lignocellulosic biomass: different activation routes and their application to dyes adsorption. J. Environ. Chem. Eng. 7, 103148.

Mbarki, F., Selmi, T., Kesraoui, A., Seffen, M., Gaddoneix, O., Celzard, A., Fierro, V., 2019. Hydrothermal pre-treatment, an efficient tool to improve activated carbon performances. Ind. Crop. Prod. 140, 111717.

Meerbergen, K., Willems, K.A., Dewil, R., Impe, J.V., Appels, L., Lievens, B., 2018. Isolation and screening of bacterial isolates from wastewater treatment plants to decolorize azo dyes. J. Biosci. Bioeng. 125, 448−456.

Mishra, S., Mohanty, P., Maiti, A., 2019. Bacterial mediated bio-decolourization of wastewater containing mixed reactive dyes using jack-fruit seed as co-substrate: process optimization. J. Clean. Prod. 235, 21−33.

Módenes, A.N., Hinterholz, C.L., Neves, C.V., Sanderson, K., Trigueros, D.E.G., Espinoza-Quiñones, F.R., Borba, C.E., Steffen, V., Scheufele, F.B., Kroumov, A.D., 2019. A new alternative to use soybean hulls on the adsorptive removal of aqueous dyestuff. Biores. Technol. Rep. 6, 175−182.

Moghazy, R.M., Labena, A., Husien, S., 2019. Eco-friendly complementary biosorption process of methylene blue using micro-sized dried biosorbents of two macro-algal species (Ulva fasciata and Sargassum dentifolium): full factorial design, equilibrium, and kinetic studies. Int. J. Biol. Macromol. 134, 330−343.

Muntean, S.G., Todea, A., Bakardjieva, S., Bologa, C., 2017. Removal of non benzidine direct red dye from aqueous solution by using natural sorbents: beech and silver fir. Desalin. Water Treat. 66, 235−250.

Murthy, T.P.K., Gowrishankar, B.S., Prabha, M.N.C., Kruthi, M., Krishna, R.H., 2019. Studies on batch adsorptive removal of malachite green from synthetic wastewater using acid treated coffee husk: equilibrium, kinetics and thermodynamic studies. Microchem. J. 146, 192−201.

Nasrullah, A., Saad, B., Bhat, A.H., Khan, A.S., Danish, M., Isa, M.H., Naeem, A., 2019. Mangosteen peel waste as a sustainable precursor for high surface area mesoporous activated carbon: characterization and application for methylene blue removal. J. Clean. Prod. 211, 1190−1200.

Nausad, M., Alqadami, A.A., Alothman, Z.A., Alsohaimi, I.H., Algamdi, M.S., Aldawsari, A.M., 2019. Adsorption kinetics, isotherm and reusability studies for the removal of cationic dye from aqueous medium using arginine modified activated carbon. J. Mol. Liq. 293, 111442.

Ofomaja, A.E., Ukpebor, E.E., Uzoekwe, S.A., 2011. Biosorption of Methyl violet onto palm kernel fiber: diffusion studies and multistage process design to minimize biosorbent mass and contact time. Biomass Bioenergy 35, 4112−4123.

Ouhammou, M., Lahnine, L., Mghazli, S., Hidar, N., Bouchdoug, M., Jaouad, A., Mandi, L., Mahrouz, M., 2019. Valorisation of cellulosic waste basic cactus to prepare activated carbon. J. Saudi Soc. Agricul. Sci. 18, 133−140.

Oymak, T., Eruigur, M., 2019. Effective and rapid removal of cationic and anionic dyes from aqueous solutions using Elaeagnus angustifolia L. fruits as a biosorbent. Desalin. Water Treat. 138, 257−264.

Ozhan, A., Sahin, O., Kucuk, M.M., Saka, C., 2014. Preparation and characterization of activated carbon from pine cone by microwave-induced $ZnCl_2$ activation and its effects on the adsorption of methylene blue. Cellulose 21, 2457−2467.

Pandey, R.K., Tewari, S., Tewari, L., 2018. Lignolytic mushroom Lenzites elegans WDP2: laccase production, characterization, and bioremediation of synthetic dyes. Ecotoxicol. Environ. Saf. 158, 50−58.

Plazinski, W., Rudzinski, W., Plazinska, A., 2009. Theoretical models of sorption kinetics including a surface reaction mechanism: a review. Adv. Colloid Interface Sci. 152, 2−13.

Postai, D.L., Rodrigues, C.A., 2018. Adsorption of cationic dyes using waste from fruits of Eugenia umbelliflora Berg (myrtaceae). Arabian J. Sci. Eng. 43, 2425−2440.

Rehman, R., Farooq, S., Mahmud, T., 2019. Use of Agro-waste Musa acuminata and Solanum tuberosum peels for economical sorptive removal of Emerald green dye in ecofriendly way. J. Clean. Prod. 206, 819−826.

Russo, M.E., Di Natale, F., Prigione, V., Tigini, V., Marzocchella, A., Varese, G.C., 2010. Adsorption of acid dyes on fungal biomass: equilibrium and kinetics characterization. Chem. Eng. J. 162, 537−545.

Safa, Y., Bhatti, H.N., 2011. Biosorption of direct red-31 and direct orange-26 dyes by rice husk: application of factorial design analysis. Chem. Eng. Res. Des. 89, 2566−2574.

Sen, S.K., Raut, S., Bandyopadhyay, P., Raut, S., 2016. Fungal decolouration and degradation of azo dyes: a review. Fungal Biol. Rev. 30, 112−133.

Sewu, D.D., Lee, D.S., Nguyen, T.H., Woo, S.H., 2019. Effect of bentonite-mineral co-pyrolysis with macroalgae on physicochemical property and dye uptake capacity of bentonite/biochar composite. J. Taiwan Inst. Chem. Eng. 104, 106−113.

Shamsollahi, Z., Partovinia, A., 2019. Recent advances on pollutants removal by rice husk as a bio-based adsorbent: a critical review. J. Environ. Manag. 246, 314−323.

Shao, H., Li, Y., Zheng, L., Chen, T., Liu, J., 2017. Removal of methylene blue by chemically modified defatted brown algae Laminaria japonica. J. Taiwan Inst. Chem. Eng. 80, 525−532.

Shrivastava, V.S., 2010. The biosorption of Safranine onto Parthenium hysterophorus L: equilibrium and kinetics investigation. Desalin. Water Treat. 22, 146−155.

Sinha, S., Singh, R., Chaurasia, A.K., Nigam, S., 2016. Self-sustainable Chlorella pyrenoidosa strain NCIM2738 based photo bioreactor for removal of Direct Red-31 dye along with other industrial pollutants to improve the water-quality. J. Hazard Mater. 306, 386−394.

Spagnoli, A.A., Giannakoudakis, D.A., Bashkova, S., 2017. Adsorption of methylene blue on cashew nut shell based carbonsactivated with zinc chloride: the role of surface and structural parameters. J. Mol. Liq. 229, 465−471.

Sudaryanto, Y., Hartono, S.B., Irawaty, W., Hindarso, H., Ismadji, S., 2006. High surface area activated carbon prepared from cassava peel by chemical activation. Bioresour. Technol. 97, 734−739.

Sun, W., Sun, W., Wang, Y., 2019. Biosorption of Direct Fast Scarlet 4BS from aqueous solution using the green-tide-causing marine algae Enteromorpha prolifera. Spectrochim. Acta Mol. Biomol. Spectrosc. 223, 117347.

Sun, Z., Srinivasakannan, C., Liang, J., Duan, X., 2019. Preparation and characterization of shiitake mushroom-based activated carbon with high adsorption capacity. Arabian J. Sci. Eng. 44, 5443−5456.

Tan, C.Y., Li, G., Lu, X.Q., Chen, Z.L., 2010. Biosorption of basic orange using dried *A. filiculoides*. Ecol. Eng. 36, 1333−1340.

Wakkel, M., Khiari, B., Zagrouba, F., 2019. Textile wastewater treatment by agro-industrial waste: equilibrium modelling, thermodynamics and mass transfer mechanisms of cationic dyes adsorption onto low-cost lignocellulosic adsorbent. J. Taiwan Inst. Chem. Eng. 96, 439−452.

Yang, J.X., Hong, G.B., 2018. Adsorption behavior of modified Glossogyne tenuifolia leaves as a potential biosorbent for the removal of dyes. J. Mol. Liq. 252, 289−295.

Yu, X., Han, Z., Fang, S., Chang, C., Han, X., 2019. Optimized preparation of high value-added activated carbon and its adsorption properties for methylene blue. Int. J. Chem. React. Eng. 17, 20180267.

Zhou, Y., Lu, J., Zhou, Y., Liu, Y., 2019. Recent advances for dyes removal using novel adsorbents: a review. Environ. Pollut. 252, 352−365.